



# Optics Letters

## Soliton-sinc optical pulses

SERGEI K. TURITSYN,<sup>1,2,\*</sup>  STEPAN BOGDANOV,<sup>2</sup> AND ALEXEY REDYUK<sup>2,3</sup>

<sup>1</sup>Aston Institute of Photonic Technologies, Aston University, Birmingham B4 7ET, UK

<sup>2</sup>Aston-NSU Center for Photonics, Novosibirsk State University, Novosibirsk 630090, Russia

<sup>3</sup>Federal Research Center for Information and Computational Technologies, Novosibirsk 630090, Russia

\*Corresponding author: s.k.turitsyn@aston.ac.uk

Received 13 July 2020; revised 22 August 2020; accepted 22 August 2020; posted 24 August 2020 (Doc. ID 402286); published 21 September 2020

**We introduce a new, to the best of our knowledge, type of band-limited optical pulse—soliton-sinc tailored to the nonlinear Schrödinger (NLS) equation. The idea behind the soliton-sinc pulse is to combine, even if approximately, a property of a fundamental soliton to propagate without distortions in nonlinear systems governed by the NLS equation with a compact band-limited spectrum of a Nyquist pulse. Though the shape preserving propagation feature is not exact, such soliton-sinc pulses are more robust against nonlinear signal distortions compared to a Nyquist pulse.** © 2020 Optical Society of America

<https://doi.org/10.1364/OL.402286>

In many physical problems we deal with band-limited fields. This can be due to the high level of loss outside of some spectral window or artificially induced filtering of a signal. Band-limited analysis can be applied to both temporal and spatial signals with an appropriate change of notations. Here we focus on the temporal domain; however, the same idea can be applied to spatial nonlinear problems.

In linear band-limited systems, the special role is played by seminal Nyquist pulses, also known as sinc pulses. Nyquist pulses possessing a rectangular frequency spectrum and having no inter-symbol interference (ISI) present the mathematical foundation of digital communications [1–3]. For continuous temporal signals, the frequency spectrum of the rectangular pulse corresponds to a sinc-shaped pulse in the time domain:  $\sin(kt)/(kt)$ . The rectangular shape of the spectrum makes Nyquist pulses particularly attractive for communication, providing for a dense packaging of the information in the spectral domain, important for efficient wave-division multiplexing.

An important trait of the Nyquist pulses is the location of the zero crossings that allows them to avoid ISI. Sinc pulse decays as  $1/|t|$  at large  $|t|$ , which makes their practical implementation challenging. Practical application of a Nyquist pulse requires some sort of smoothening of sharp mathematical conditions at the edges of the spectrum at the expense of broadening the transition region. There are various implementations of Nyquist pulses in practice, such as, e.g., raised-cosine pulse, root-raised cosine (RRC) [4], and also various improved Nyquist pulses [5,6].

The classical theory of communication assumes that the spectral bandwidth of the signal is not changed during transmission. This assumption is evidently justified in linear channels; however, nonlinear effects might break this basic conjecture. The optical fiber is a well-known example of a nonlinear (when the accumulated nonlinear phase shift is large enough) system, with enormously high bandwidth. The propagating field with the initial spectrum—much narrower than the whole window of fiber transparency—can experience substantial spectral broadening, leading to fascinating physical effects such as, e.g., formation of a supercontinuum [7,8]. In general, optical fiber communications is governed by nonlinear channels that deviate from the classical linear white-Gaussian noise channels in which sinc pulses are widely used. Nonlinear propagation effects lead to signal distortions that are absent in linear systems. Carrier pulses (like sincs) that are optimal in linear channels are affected by nonlinearity that not only deforms signal shape, but also breaks orthogonality, leading to ISI. This effect is especially profound at high signal powers. Therefore, the search for optimal carrier pulse shaping in nonlinear channels is still ongoing. A nonlinear fiber channel can be approximated in certain limits by the nonlinear Schrödinger (NLS) equation with additive noise [9]. The NLS equation is an example of the nonlinear model integrable by the inverse scattering transform [10]. Moreover, the NLS equation is a very generic nonlinear model that occurs in different areas of science (see e.g., [9,11–14] and numerous references therein). Therefore, we consider here the NLS equation as a master nonlinear model to illustrate the general concept that can be applied in various areas.

In this Letter, we consider propagation of a band-limited field in the nonlinear system governed by the NLS equation with a much broader spectral range compared to the initial signal bandwidth. We compare nonlinear spectral distortions for several band-limited pulses. We introduce a new family of band-limited pulses that have propagation properties adjusted to the NLS equation—soliton-sinc pulses. Though the proposed signal waveform potentially might be useful in communication systems covered by the NLS equation model, we focus in this Letter on the general properties of such pulses that might have applications in different areas.

Without loss of generality, we use here terminology corresponding to temporal signal evolution with distance, similar to

the case of nonlinear fiber optics. The seminal NLS equation, written in the normalized form

$$i \frac{\partial A}{\partial z} + \frac{1}{2} \frac{\partial^2 A}{\partial t^2} + |A|^2 A = 0, \quad (1)$$

has a well-known fundamental soliton solution [sech( $x$ ) = 1/cosh( $x$ ) notation often is used in the soliton community]:

$$A_{\text{sol}}(t, z) = \frac{1}{\tau} \frac{\exp[iz/(2\tau^2)]}{\cosh(t/\tau)} = \frac{1}{\tau} \times \exp\left[\frac{iz}{2\tau^2}\right] \times \text{sech}\left(\frac{t}{\tau}\right).$$

Soliton pulse width at half maximum is expressed through the parameter  $\tau$  as  $T_{\text{FWHM}} \approx 1.76\tau$ . A normalized soliton energy  $E_{\text{sol}} = \int |A_{\text{sol}}|^2 dt = 2/\tau$ . It is well known that a soliton pulse propagates in the systems governed by Eq. (1) without distortion of its shape despite nonlinearity. The key idea behind the proposed soliton-sinc pulse is to have a band-limited signal, while trying to preserve as much as possible the robustness inherent to solitons during propagation in nonlinear media described by the NLS model.

We consider for comparison the normalized soliton pulse, introduced above, and sinc pulse  $A_{\text{sinc}}$  with intensity

$$I_{\text{sinc}}(t) = I_0 \times \frac{\sin^2(Bt/2)}{B^2 t^2/4}.$$

Spectral power for the normalized (as above) soliton reads

$$I_{\text{sol}}(\omega) = |A_{\text{sol}}(\omega)|^2 = \frac{1}{4 \cosh^2(\omega\pi\tau/2)}.$$

We introduce soliton-sinc pulse  $A_{SS}(\omega)$  in the frequency domain in the following way. Soliton-sinc has a soliton shape ( $A_{SS}(\omega) = 0.5 \text{sech}(\omega\pi\tau/2)$ ) in the interval  $|\omega| \leq B/2$  (soliton feature) and has zero power elsewhere:  $A_{SS}(\omega) = 0$ , when  $|\omega| > B/2$  (Nyquist pulse characteristic). Respectively, in the time domain, soliton-sinc takes the form

$$A_{ss}(t, t_0, B) = \frac{1}{2} \int_{-B/2}^{B/2} \frac{\exp(-i\omega t)}{\cosh(\omega t_0)} d\omega = \frac{1}{2t_0} f_{ss}\left(\frac{t}{t_0}, Bt_0\right), \quad (2)$$

where  $t_0 = \pi\tau/2 \approx 1.57\tau$ , and the dimensionless soliton-sinc waveform is defined by the function of two variables,  $x = t/t_0$  and  $y = Bt_0$ :

$$f_{ss}(x, y) = \int_{-y/2}^{y/2} \frac{\exp(-isx)}{\cosh(s)} ds.$$

Figures 1(a) (time domain) and 1(b) (spectrum) depict three pulses of the same energy: Nyquist pulse (dashed blue line), soliton (short-dashed red), and soliton-sinc (solid black). Both sinc and soliton-sinc have characteristic oscillating tails. Here, the soliton parameter  $\tau = 1.0$ , which corresponds to  $t_0 \approx 1.57$ .

Figure 2 depicts the soliton-sinc waveform  $A_{ss}(t, t_0)$  for  $B = 2.9$  and varying  $t_0$ . It is seen that as  $t_0$  changes from zero to a large value, the soliton-sinc shape evolves from the Nyquist pulse to a pure soliton. Four same-energy pulses shown in the lower part of Fig. 2 correspond to the different values of  $t_0 = 0.75, 1.5, 2.25,$  and  $3.0$ . Though unlike for Nyquist pulses we do not expect the orthogonality and zero ISI for soliton-sincs, it might be beneficial to suppress ISI between at least the

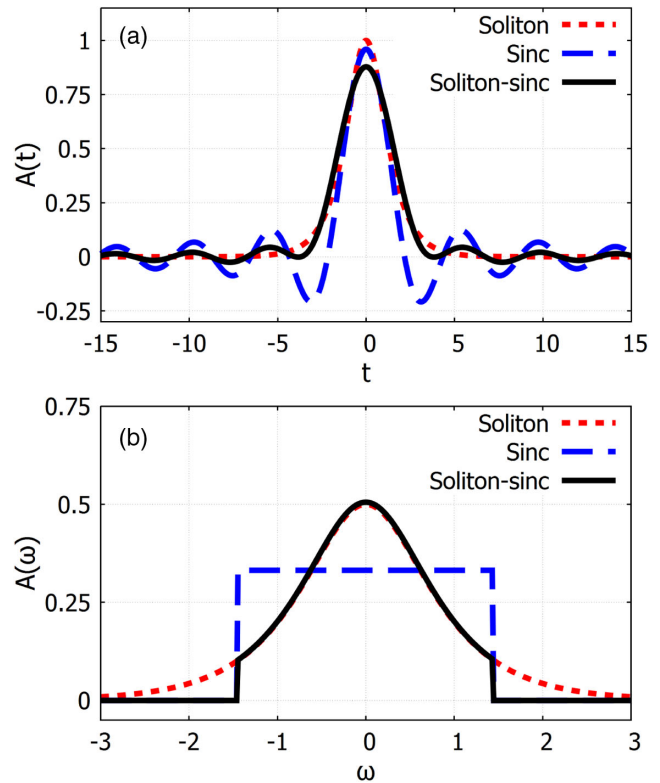
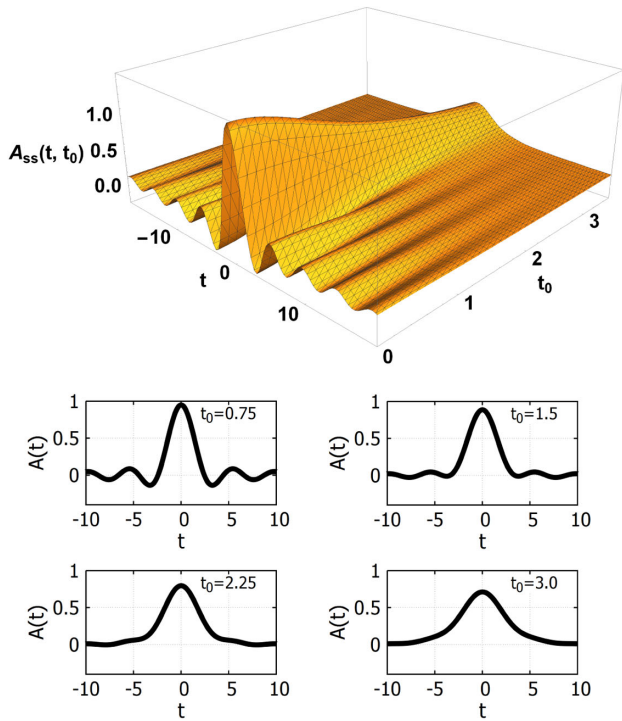


Fig. 1. Normalized sinc (dashed blue), soliton (short-dashed red), and soliton-sinc (solid black) pulses in: (a) time domain and (b) spectral domain. Here  $B = 2.9$ .

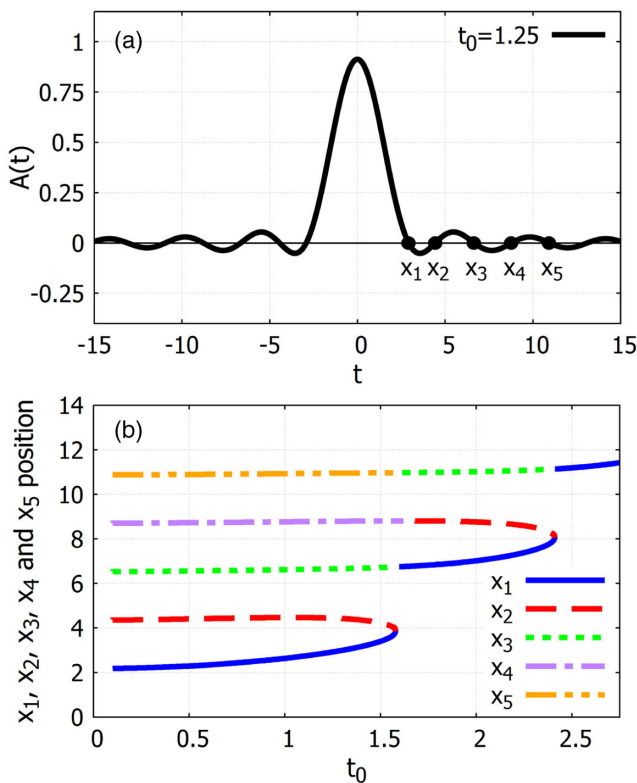
first several neighboring pulses. Therefore, we examine now the positions of the first zeros  $x_k$  of the equation  $f_{ss}(x_k, y) = 0$ , as shown in Fig. 3. This implicit equation has solutions  $x_k = g(y)$ , and, respectively,  $t_k = t_0 g(Bt_0)$  depends on  $t_0$  and  $B$ . Using these two parameters, it is possible to manipulate positions of zeros. For instance, considering the distance between two neighboring soliton-sincs to be  $T$  (and similar to sinc, assuming  $T = 1/B$ ), we get  $t_k = t_0 g(Bt_0) = T = 1/B$ , which defines, for each index  $k$ , implicitly  $\tau = h(B)$ , which ensures that soliton-sinc zeros are located at the neighboring pulse maximum. To be able to change the amplitude of soliton-sinc (defined by  $\tau$ ) while holding the condition that zero in the oscillating wing is in the center of the neighboring time slot, we can use second and third zeros.

Figure 3(a) shows a normalized soliton-sinc pulse with  $t_0 = 1.25, B = 2.9$  (the choice of  $B$  is somewhat arbitrary;  $B = 2.9$  for  $\tau = 1$  is close to the bifurcation condition  $x_1 = x_2$ ). Points  $x_k = t_k/t_0$  with  $k = 1, 2, 3, 4, 5$  correspond to zeros of the soliton-sinc. Figure 3(b), which is a cross section of Fig. 2 (top) defined by  $|A_{ss}(t_k, t_0)| = 0$ , depicts positions of zeros as functions of the parameter  $t_0$ . A tongue-like structure of solutions with bifurcation points corresponding to the convergence of two branches makes  $x_k$  piece-wise functions of  $t_0$ .

In the NLS equation, any initial pulse without temporal phase variation asymptotically evolves into a soliton provided that the condition  $\int |A(t, z=0)| dt > \pi/2$  is satisfied [15]. However, we consider here propagation distances shorter than required for soliton formation. During this intermediate stage of nonlinear evolution, the waveform and the spectrum of the signal can be changed dramatically from the initial ones. To



**Fig. 2.** Temporal shapes of a soliton-sinc pulse  $A_{ss}(t, t_0)$  for  $B = 2.9$  and varying  $t_0$ . Upper figure shows evolution of the soliton-sinc shape from pure sinc (at  $t_0 = 0$ ) to soliton (in the limit of large  $t_0$ ). Four figures below depict projections of the upper at fixed  $t_0 = 0.75, 1.5, 2.25,$  and  $3.0$ .



**Fig. 3.** (a) Soliton-sinc pulse and its five first zeros,  $B = 2.9$ . (b) Dependence of  $x_k, k = 1, 2, 3, 4, 5$  on the parameter  $t_0$ .

illustrate the relative robustness of the soliton-sinc during nonlinear propagation, we compare its spectral dynamics to sinc and RRC waveform, often used as a practical approximation of the Nyquist pulse. The RRC pulse is defined as [4]

$$A_{RRC}(\omega) = \begin{cases} 1, & |\omega| \leq \frac{(1-\rho)}{2T_s} \\ \cos \left[ \frac{\pi T_s}{2\rho} \left( |\omega| - \frac{(1-\rho)}{2T_s} \right) \right], & \frac{(1-\rho)}{2T_s} < |\omega| < \frac{(1+\rho)}{2T_s} \\ 0, & \text{else} \end{cases} \quad (3)$$

where  $T_s = 1/B$  is the time slot, and  $\rho$  is the roll-off factor.

Figure 4 shows nonlinear evolution with distance  $z$  of the power spectral density of Nyquist [Fig. 4(a)], RRC [Fig. 4(b)], and soliton-sinc [Fig. 4(c)] pulses (same energy). It is seen that both Nyquist and RRC pulses undergo substantial deformation from their initial rectangular shape into oscillating breather-like spectra, while soliton-sinc experiences similar, but visibly smaller, distortions of the spectrum, holding approximately the same spectral shape. Note that the spectral energy leakage outside the initial bandwidth for soliton-sinc is slightly

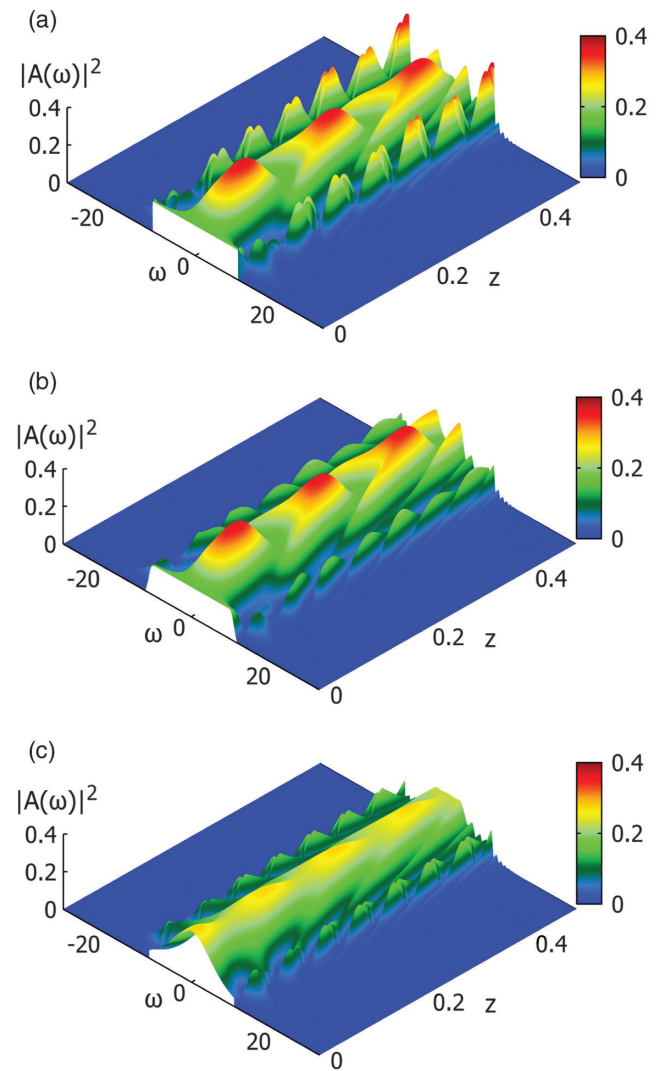


**Fig. 4.** Evolution of the power spectral density  $|A(z, \omega)|^2$  for the Nyquist pulse (a); RRC pulse (roll-off factor  $\rho = 0.1$ ) (b); soliton-sinc pulse (c). Here  $\tau = 1/10, B = 20$ .

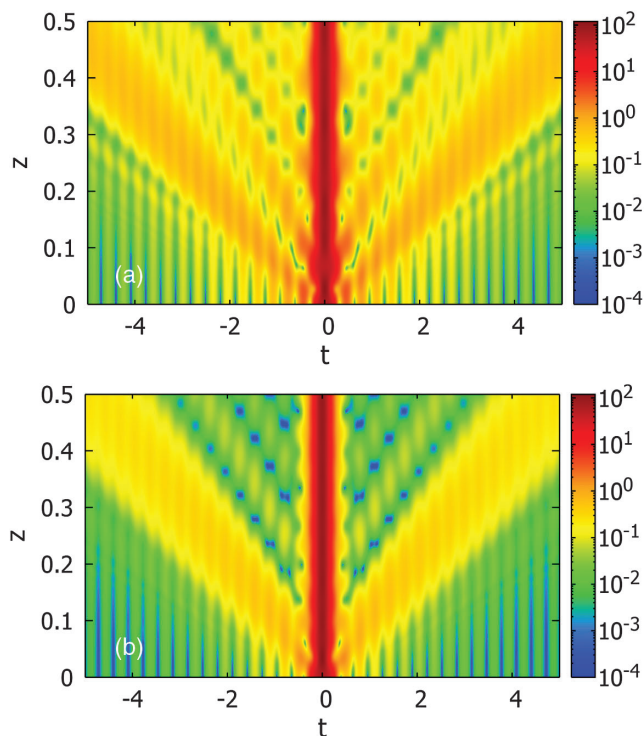


**Fig. 5.** Temporal evolution of sinc pulse power  $|A(t, z)|^2$  (a) and soliton-sinc (b) shown in the logarithmic scale. Here  $\tau = 1/10$ ,  $B = 20$ .

smaller compared to sinc and RRC pulses. Figure 4(c) illustrates soliton-sinc's ability both to hold a spectral shape of the energy-containing core during evolution and retain a compact bandwidth. This feature might be useful for high-power applications under constraint of a compact bandwidth.

Similar reduced nonlinear distortions of soliton-sinc compared to the sinc (and RRC) pulse are observed in the temporal domain. Figure 5 compares temporal dynamics of sinc [Fig. 5(a)] and soliton-sinc [Fig. 5(b)]. Though both pulses experience nonlinear distortions, especially during the stage of transition from the initial pulse, overall, soliton-sinc demonstrates more stable temporal dynamics with reduced nonlinear deformation. The dynamics of RRC pulse is close to the one of sinc and is not shown here.

A conventional fundamental soliton is formed through the balance between nonlinearity and dispersion (in temporal solitons) or diffraction (in spatial solitons). A soliton is a remarkable example of how nonlinear properties of the physical medium can be positively utilized to create a robust coherent localized structure. However, the NLS equation model assumes, formally speaking, infinite, and, in practical terms, a large (compared to the spectral interval where most of the energy is located) bandwidth of the medium in which such soliton propagates. Thus, a pure NLS equation soliton is affected by narrow spectral filtering (for temporal solitons) or a diaphragm (in a spatial soliton beam case).

Any initial localized field distribution having appropriate energy evolves into a soliton in a long enough medium.

Mathematically speaking, for soliton formation, the Zakharov–Shabat spectral problem [10] solved for a particular initial field should have a single eigenvalue that corresponds to a soliton solution to the NLS equation. However, when the propagation distance is smaller compared to the typical soliton formation length, it is of interest to find intermediate regimes of stable nonlinear dynamics with effectively limited bandwidth.

We introduced here a new class of the band-limited pulses—soliton-sinc—tailored to the NLS equation. The proposed pulse inherits from a fundamental soliton a nonlinear tolerance (though a pure shape preserving property of the soliton is replaced in the heir—soliton-sinc pulse—by a reduced level of nonlinear distortions) and has a limited bandwidth of a Nyquist pulse. Though the shape preserving propagation feature is not exact, the proposed soliton-sinc pulses are more robust against nonlinear distortion during propagation compared to pure sincs. Nonlinear pulse shaping using optical fiber dynamics is a fascinating area of research (see, e.g., [16–18] and references therein), and band-limited nonlinear pulses can be an interesting new direction. We anticipate that the proposed pulse might find applications in different fields where the NLS equation is used as a master model.

**Funding.** Russian Science Foundation (Grant No. 17-72-30006).

**Disclosures.** The authors declare no conflicts of interest.

## REFERENCES

- H. Nyquist, *Trans. Am. Inst. Electr. Eng.* **47**, 617 (1928).
- V. V. Kotelnikov, in *Material for the First All-Union Conference on Questions of Communication (in Russian)* (Izd. Red. Upr. Svyazi RSKA, 1933).
- C. E. Shannon, *Bell Syst. Tech. J.* **27**, 379 (1948).
- J. G. Proakis, *Digital Communications*, 4th ed. (McGraw-Hill, 2000).
- A. Assalini and A. M. Tonello, *IEEE Commun. Lett.* **8**, 87 (2004).
- B. Châtelain, C. Laperle, K. Roberts, M. Chagnon, X. Xu, A. Borowiec, F. Gagnon, and D. V. Plant, *Opt. Express* **20**, 8397 (2012).
- J. M. Dudley, G. Genty, and S. Coen, *Rev. Mod. Phys.* **78**, 1135 (2006).
- S. Smirnov, J. Ania-Castanon, T. Ellingham, S. Kobtsev, S. Kukarin, and S. Turitsyn, *Opt. Fiber Technol.* **12**, 122 (2006).
- L. F. Mollenauer and J. P. Gordon, *Solitons in Optical Fiber* (Academic, 2006), Vol. **10**, p. 486.
- V. E. Zakharov and A. B. Shabat, *J. Exp. Theor. Phys.* **34**, 62 (1972).
- M. Remoissenet, *Waves Called Solitons: Concepts and Experiments*, Advanced Texts in Physics (Springer, 1999).
- Y. Kivshar and G. Agrawal, *Optical Solitons: From Fibers to Photonic Crystals* (Elsevier, 2003).
- S. Trillo and W. Torruellas, *Spatial Solitons*, Springer Series in Optical Sciences (Springer, 2013).
- S. K. Turitsyn, B. G. Bale, and M. P. Fedoruk, *Phys. Rep.* **521**, 135 (2012).
- M. Klaus and J. K. Shaw, *SIAM J. Math. Anal.* **34**, 759 (2003).
- S. Boscolo and C. Finot, *Int. J. Opt.* **2012**, 159057 (2012).
- J. Azaña, L. Oxenløwe, E. Palushani, R. Slavik, M. Galili, H. Mulvad, H. Hu, Y. Park, A. Clausen, and P. Jeppesen, *Int. J. Opt.* **2012**, 1 (2012).
- S. Boscolo, A. Latkin, and S. Turitsyn, *IEEE J. Quantum Electron.* **44**, 1196 (2008).